TN 1633

NACA TN No. 1633

NATIONAL ADVISORY COMMITTEE FOR AERONAUTICS

TECHNICAL NOTE

No. 1633

AN EVALUATION OF THE CHARACTERISTICS OF A 10-PERCENT-THICK NACA 66-SERIES AIRFOIL SECTION WITH A SPECIAL MEAN-CAMBER LINE DESIGNED TO PRODUCE A HIGH CRITICAL MACH NUMBER

By Laurence K. Loftin, Jr., and Kenneth S. Cohen

Langley Aeronautical Laboratory
Langley Field, Va.

Washington
July 1948

NATIONAL ADVISORY COMMITTEE FOR AERONAUTICS

TECHNICAL NOTE NO. 1633

AN EVALUATION OF THE CHARACTERISTICS OF A 10-PERCENT-THICK NACA 66-SERIES AIRFOIL SECTION WITH A SPECIAL MEAN-CAMBER LINE DESIGNED TO PRODUCE A HIGH CRITICAL MACH NUMBER

By Laurence K. Loftin, Jr., and Kenneth S. Cohen

SUMMARY

The low-speed aerodynamic characteristics of the NACA $66_{(09)}\text{-}210 \left\{\begin{matrix} a = 1.0, & c_{l_i} = 0.6 \\ a = 0.6, & c_{l_i} = -0.4 \end{matrix}\right\}$ airfoil section were determined from tests in the Langley two-dimensional low-turbulence pressure tunnel. These data and similar data for the NACA 66-210,a=1.0 airfoil are presented. By the use of these low-speed data and high-speed data obtained in the Ames 1- by $3\frac{1}{2}$-foot high-speed tunnel, a comparison of the NACA $66_{(09)}\text{-}210 \left\{\begin{matrix} a = 1.0, & c_{l_i} = 0.6 \\ a = 0.6, & c_{l_i} = -0.4 \end{matrix}\right\}$ and NACA 66-210,a=1.0 airfoils was made at both low and high speeds. The high-speed data indicated that the airfoil with the special mean line had a drag-divergence Mach number at the design lift coefficient slightly higher than that of the NACA 66-210,a=1.0 airfoil section, but this increase was not so great as that shown by calculations based on low-speed data of the critical Mach numbers for the two airfoils. With the exception of a negative increase of about 50 percent in the pitching moment, the low-speed characteristics of the airfoil with the special mean line were in essential agreement with those of the same airfoil having the a = 1.0 mean line.

INTRODUCTION

The mean-camber line of an airfoil may be so designed that the induced velocities resulting from the camber will occur over that part of the airfoil chord along which the induced velocities resulting from the basic thickness form are small. Thus, by a proper combination of mean line and basic thickness form, the critical Mach number of a cambered airfoil may be increased above that usually predicted for an airfoil cambered with a more conventional-type mean line such as the a = 1.0.

Lift was measured by taking the difference betweeen the pressure reaction upon the floor and ceiling of the tunnel; drag was determined by the wake-survey method; and pitching moments were measured by a torque balance. Measurements of the pressure distribution about the airfoil were made by means of small pressure orifices located on the upper and lower surfaces of the model midway between the vertical walls of the tunnel. A more complete description of the tunnel and the methods of obtaining and reducing the data are contained in reference 4.

Lift, drag, and pitching-moment measurements were made for the plain airfoil in the smooth condition at Reynolds numbers of 3.0×10^6, 6.0×10^6, and 9.0×10^6. The lift and moment characteristics of the airfoil equipped with a simulated split flap deflected 60° were measured at a Reynolds number of 6.0×10^6. In order to show the effect of surface condition upon the aerodynamic characteristics, lift and drag tests of the airfoil were made with standard roughness applied to the leading edge of the model. The roughness employed on the 24-inch-chord model consisted of 0.011-inch-diameter carborundum grains spread over a surface length of 0.08c behind the leading edge of the airfoil on the upper and lower surfaces. The grains were thinly spread to cover from 5 to 10 percent of this area. The pressure distributions corresponding to a range of angle of attack extending from the positive to the negative stall were determined for the smooth plain airfoil at a Reynolds number of 6.0×10^6.

RESULTS AND DISCUSSION

The influence of the tunnel boundaries has been removed from all the aerodynamic data by means of the following relations (developed in reference 4):

$$c_l = 0.974c_l'$$

$$\alpha_o = 1.015\alpha_o'$$

$$c_{m_{c/4}} = 0.989c_{m_{c/4}}'$$

$$c_d = 0.989c_d'$$

where the primed quantities represent the measured coefficients. The corrections made to the pressure data were derived on the same basis and were of the same order of magnitude as those made to the coefficients.

Critical-speed characteristics.- The critical-speed data predicted from theoretical low-speed pressure distributions by the method of reference 5 indicate that the airfoil with the special mean line has critical Mach numbers which are about 0.015 larger than those of the same airfoil with the $a = 1.0$ mean line (fig. 4). This increase is only apparent within that range of lift coefficient over which the critical Mach number varies linearly.

The center of that range of lift coefficient within which the critical Mach number varies linearly with lift coefficient changes to a value less than the theoretical design lift coefficient when the experimental rather than the theoretical low-speed pressure distributions are used for predicting the critical Mach numbers (fig. 4). The term "effective design lift coefficient" is used when referring to this experimental center. A decrease in the extent of the high critical Mach number range and an increase in the values of the critical Mach numbers within this range are also evident when the critical-speed curve predicted from the experimental pressure distribution is compared with that predicted from the theoretical pressure distributions. These same trends are noted in the results for some of the airfoils discussed in reference 1.

Some insight into the differences between the critical-speed characteristics of the airfoil as predicted from theoretical and experimental low-speed pressure distributions may be gained from figure 5. Shown in figure 5 are data representing the experimental pressure distribution for which the gradients most nearly agree over the forward part of the airfoil with those calculated theoretically for the design-lift condition. The failure of the theoretical load distribution to be realized experimentally for this condition (fig. 5) is responsible for the previously mentioned differences between the theoretical and effective design lift coefficients. A study of figure 6 indicates the formation of negative pressure peaks near the leading edge to be responsible for the short range of lift coefficient through which the critical Mach number varies linearly. The experimental peak negative pressure for the effective design-lift condition is less than that for the theoretical design lift coefficient (fig. 5), which accounts for the difference in magnitude of the critical Mach numbers corresponding to the theoretical and effective design lift coefficients (fig. 4).

The experimental pressure distributions of airfoils with the $a = 1.0$ type mean line agree quite well with those predicted theoretically (reference 3). The critical-speed characteristics of the airfoil with the special mean line, relative to those of the airfoil with the $a = 1.0$ type mean line, would seem therefore to depend upon which type of pressure distribution, theoretical or experimental, is considered as a basis for predicting the critical Mach numbers. Fortunately, in view of the confusing critical-speed results, high-speed data exist (reference 2) which permit an evaluation of the airfoil with the special mean line on the basis of drag-divergence Mach numbers. High-speed data are presented in reference 2 for a special mean-line airfoil similar to the airfoil considered in the present investigation, except that the rear

TABLE I

ORDINATES OF THE

NACA $66_{(09)}$-210 $\begin{Bmatrix} a = 1.0, & c_{l_i} = 0.6 \\ a = 0.6, & c_{l_i} = -0.4 \end{Bmatrix}$

AIRFOIL SECTION

[Stations and ordinates given in percent of airfoil chord]

Upper surface		Lower surface	
Station	Ordinate	Station	Ordinate
0	0	0	0
.475	.783	.525	-.743
.722	.944	.778	-.888
1.220	1.187	1.280	-1.101
2.469	1.590	2.531	-1.450
4.968	2.205	5.032	-1.973
7.469	2.687	7.531	-2.387
9.971	3.095	10.029	-2.741
14.975	3.752	15.025	-3.310
19.979	4.251	20.021	-3.751
24.983	4.634	25.017	-4.092
29.985	4.925	30.015	-4.349
34.986	5.135	35.014	-4.527
39.985	5.271	40.015	-4.633
44.980	5.336	45.020	-4.662
49.971	5.333	50.029	-4.611
54.955	5.265	55.045	-4.471
59.913	5.131	60.087	-4.209
64.886	4.891	65.114	-3.731
69.901	4.522	70.099	-3.094
74.934	4.029	75.066	-2.363
79.973	3.425	80.027	-1.603
85.009	2.721	84.991	-.859
90.030	1.917	89.970	-.219
95.029	1.033	94.971	-.203
100.000	0	100.000	0

L.E. radius: 0.643
Slope of radius through L.E.: 0.033

NACA

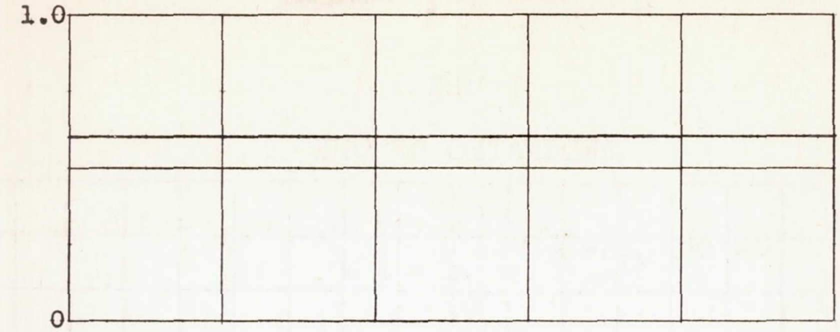

(a) Load distribution of the NACA $a = 1.0$, $c_{l_i} = 0.6$ mean line.

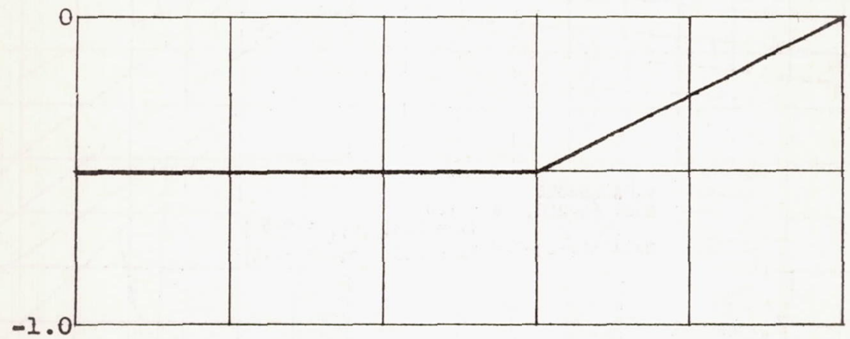

(b) Load distribution of the NACA $a = 0.6$, $c_{l_i} = -0.4$ mean line.

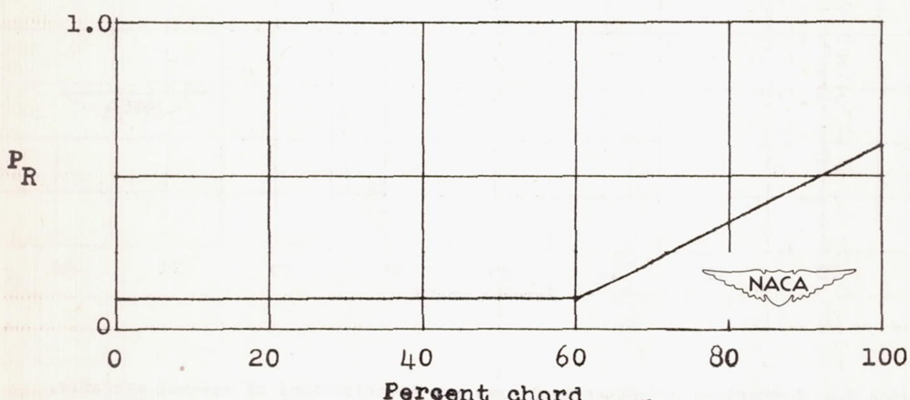

(c) Load distribution of the NACA $\left\{\begin{matrix} a = 1.0, & c_{l_i} = 0.6 \\ a = 0.6, & c_{l_i} = -0.4 \end{matrix}\right\}$ mean line (formed by superposition of the load distributions of the NACA $a = 1.0$, $c_{l_i} = 0.6$ and NACA $a = 0.6$, $c_{l_i} = -0.4$ mean lines).

Figure 1.- Load distribution of the mean line NACA $\left\{\begin{matrix} a = 1.0, & c_{l_i} = 0.6 \\ a = 0.6, & c_{l_i} = -0.4 \end{matrix}\right\}$ and component mean lines from which it is formed.

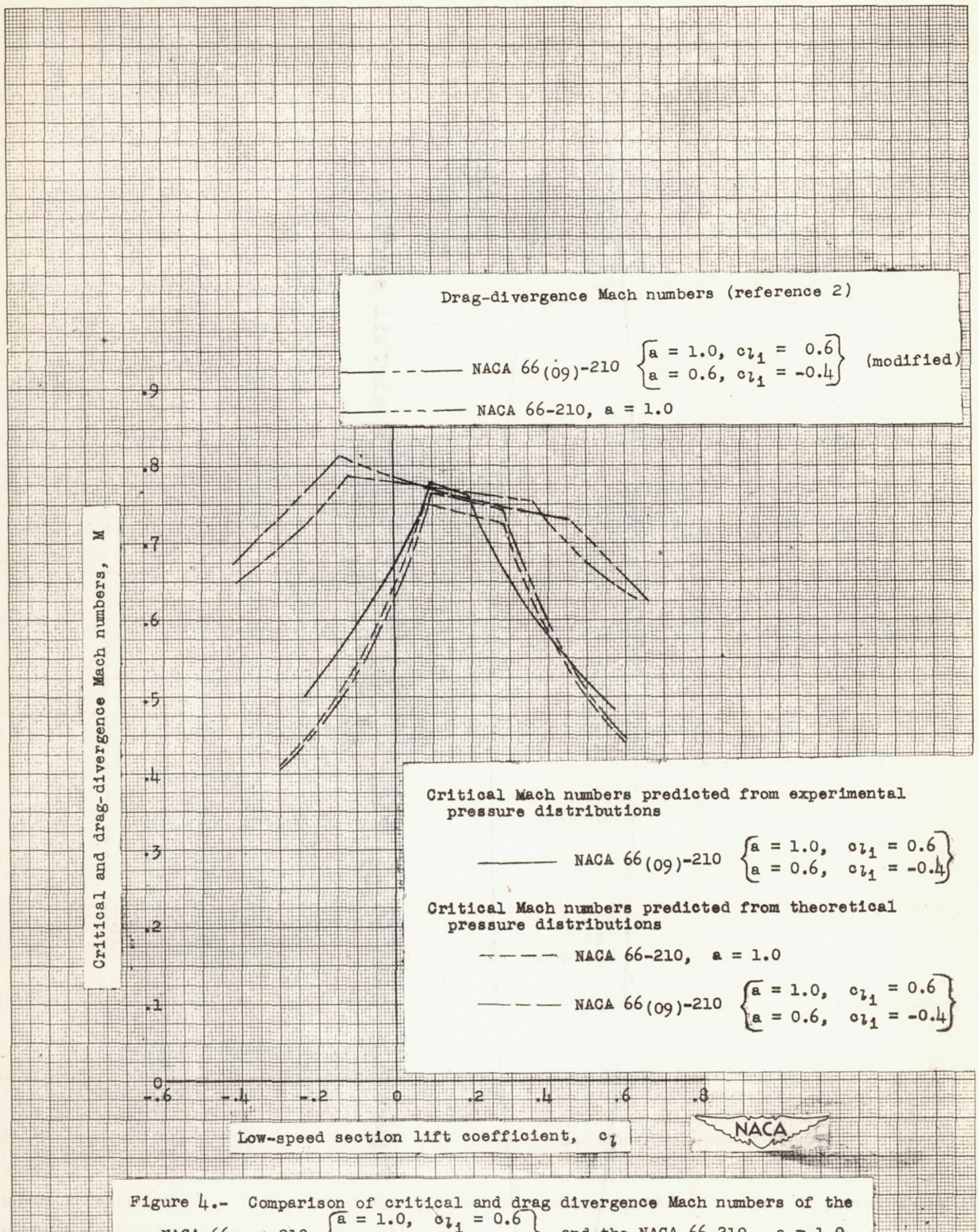

Figure 4.- Comparison of critical and drag divergence Mach numbers of the NACA 66(09)-210 $\begin{cases} a = 1.0, & c_{l_1} = 0.6 \\ a = 0.6, & c_{l_1} = -0.4 \end{cases}$ and the NACA 66-210, a = 1.0 airfoil sections.

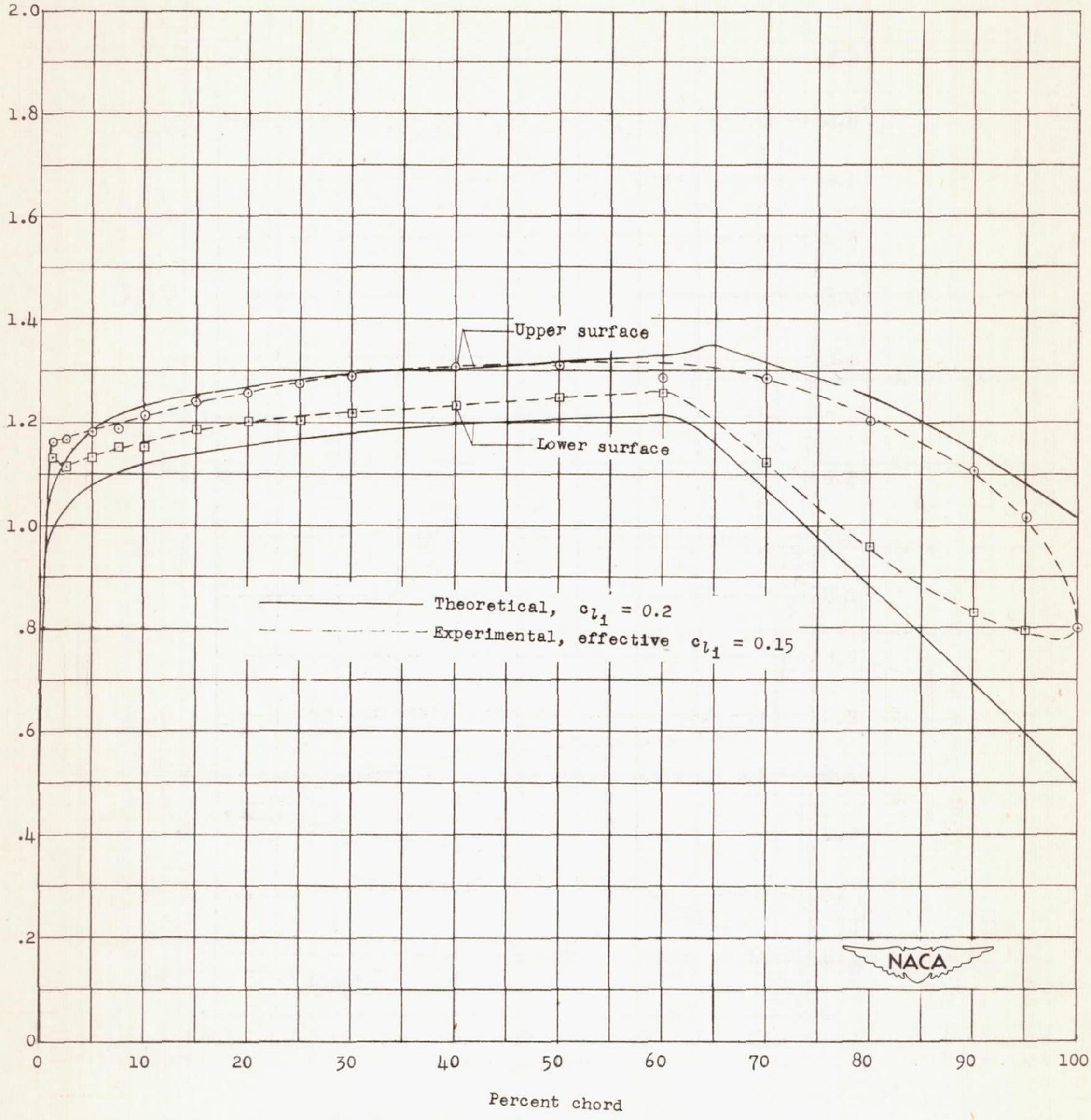

Figure 5.- Comparison of the experimental pressure distribution of the NACA 66(09)-210 $\begin{Bmatrix} a = 1.0, & c_{l_i} = 0.6 \\ a = 0.6, & c_{l_i} = -0.4 \end{Bmatrix}$ airfoil at the effective design lift coefficient with the theoretical pressure distribution at the design lift coefficient.

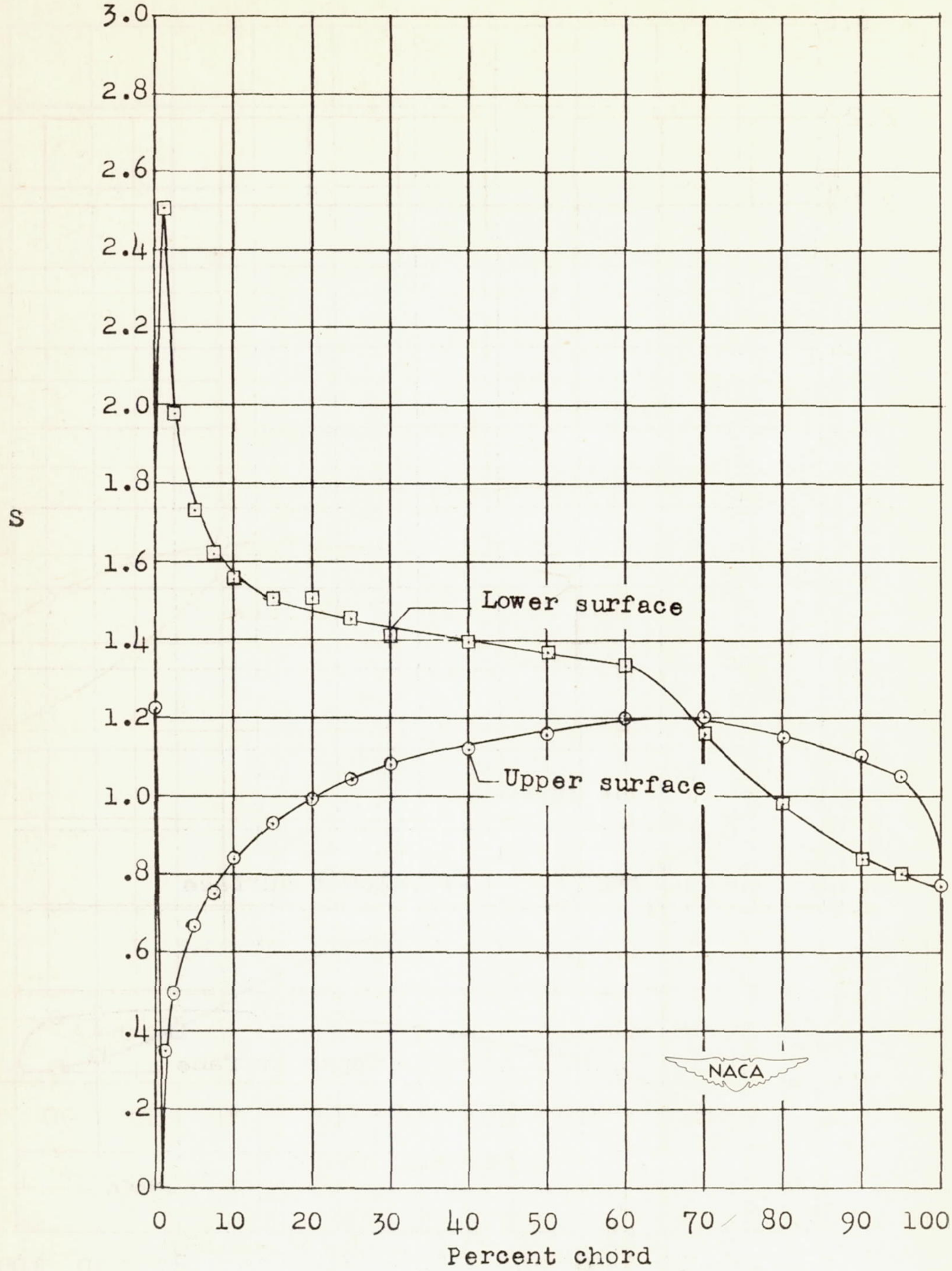

(c) $\alpha_o = -4.0^o$; $c_l = -0.24$.

Figure 6.- Continued.

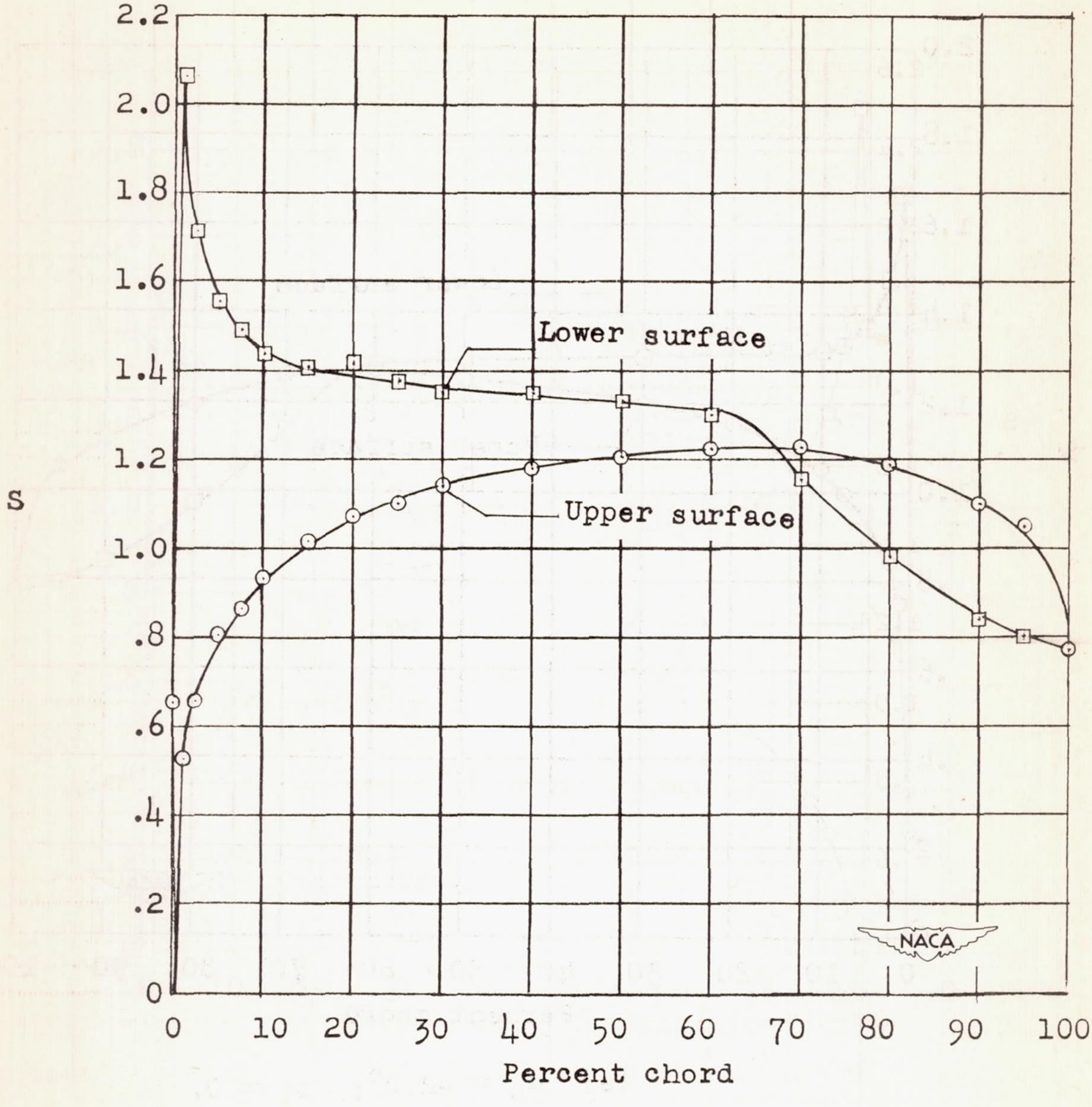

(d) $\alpha_o = -3.0^\circ$; $c_l = -0.13$.

Figure 6.- Continued.

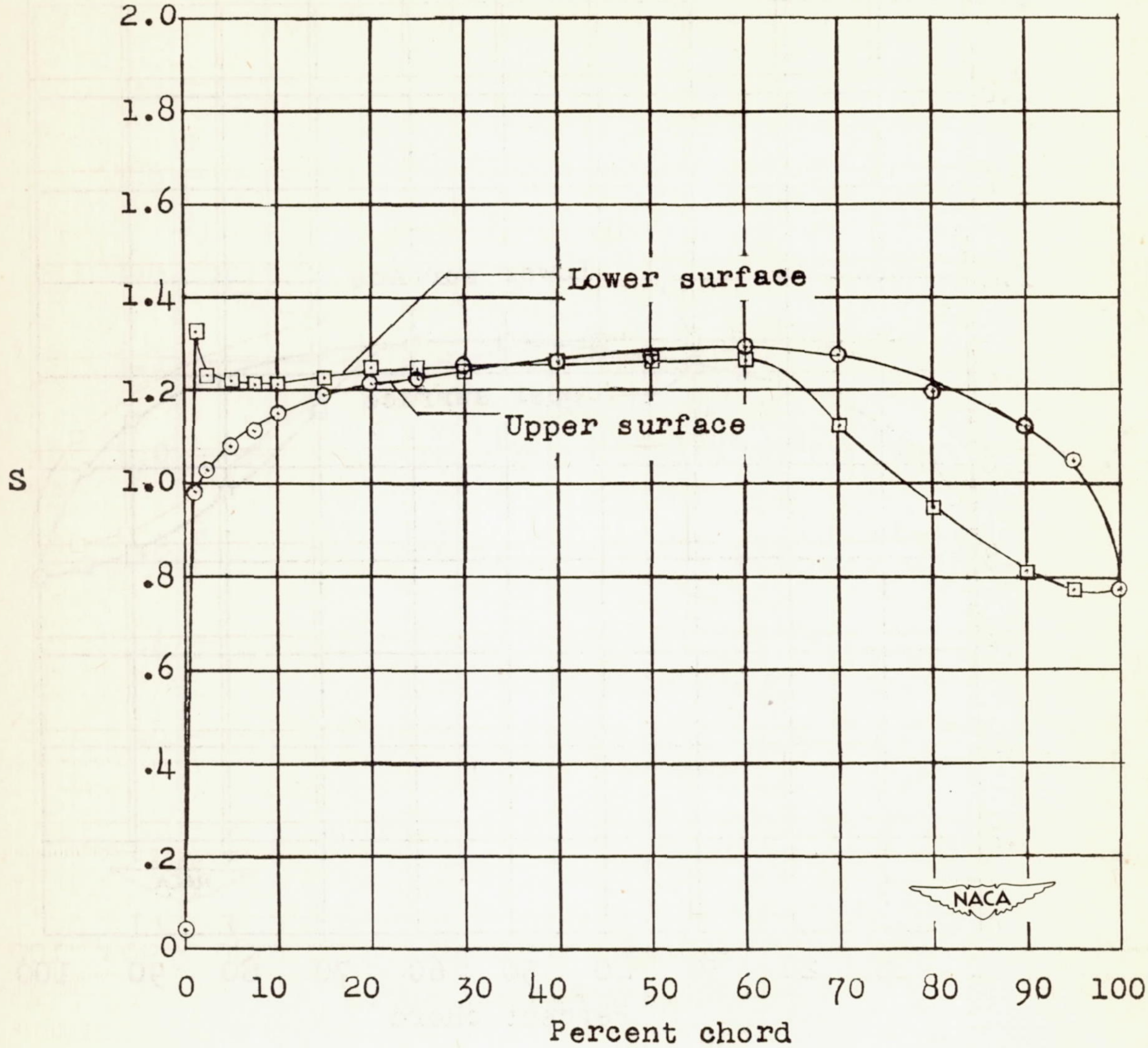

(g) $\alpha_o = -1.0$; $c_l = 0.05$.

Figure 6.- Continued.

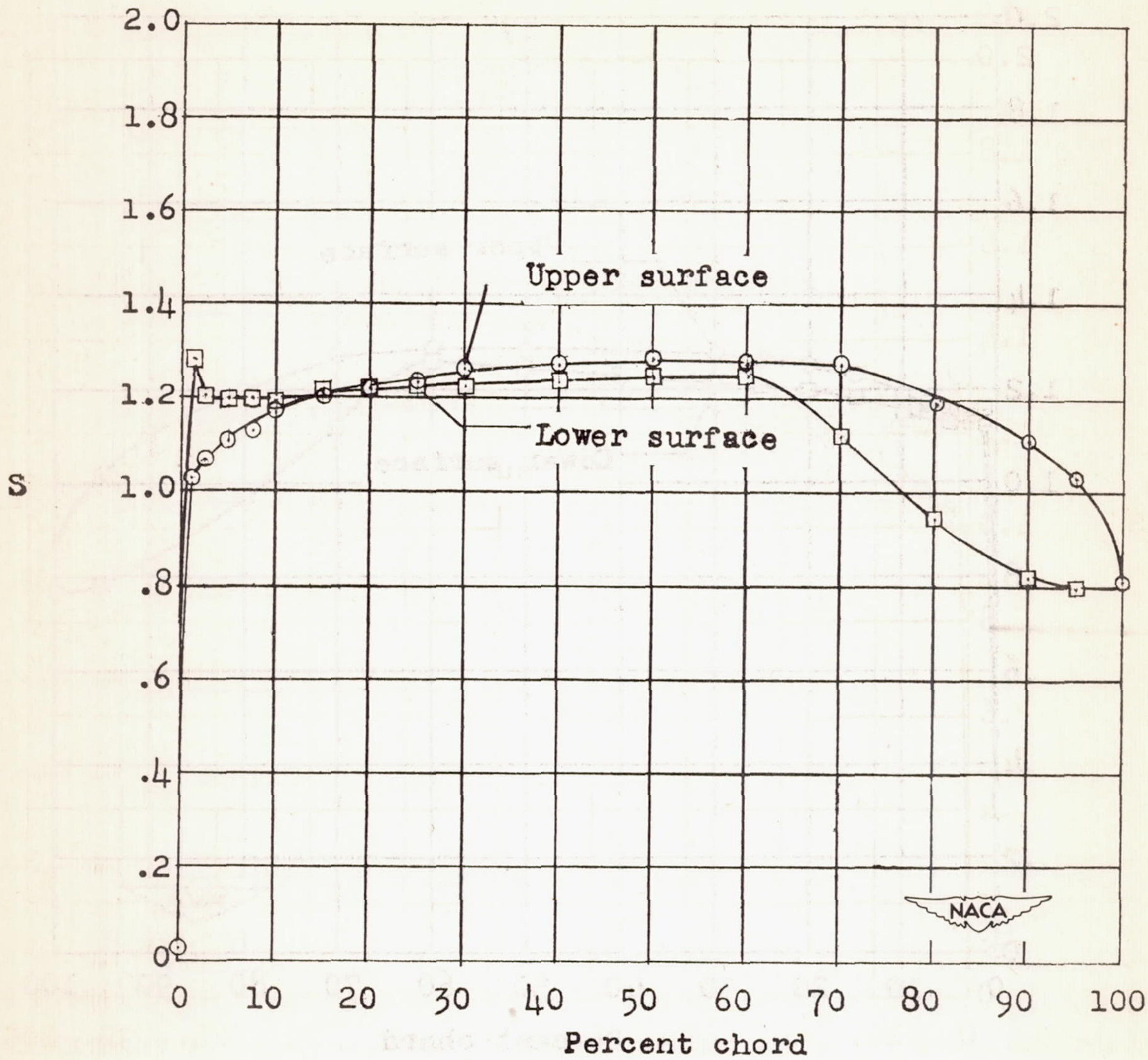

(h) $\alpha_o = -0.8^o$; $c_l = 0.08$.

Figure 6.- Continued.

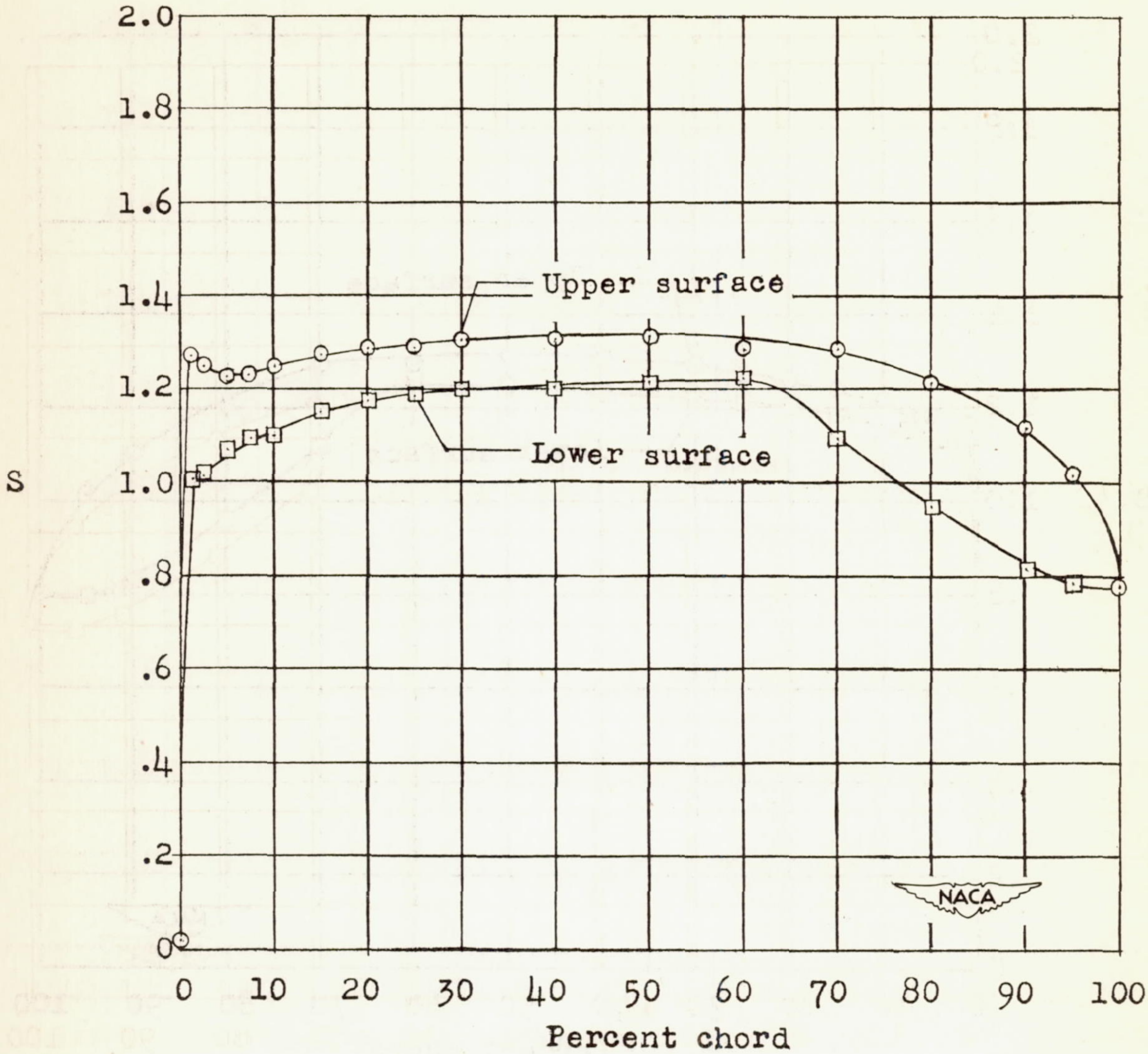

(k) $\alpha_o = 0^\circ$; $c_l = 0.18$.

Figure 6.- Continued.

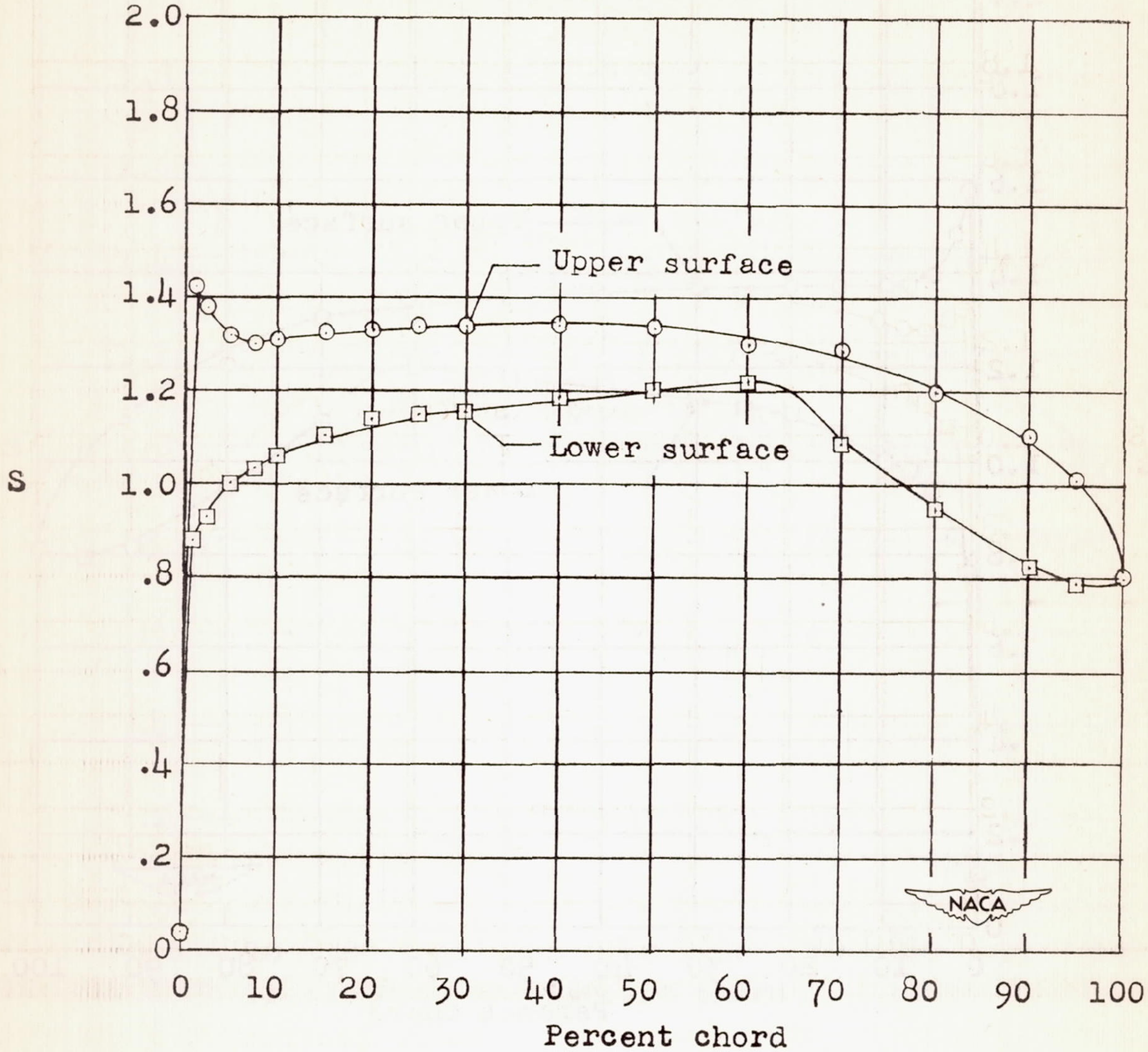

(l) $\alpha_o = 0.5^o$; $c_l = 0.23$.

Figure 6.- Continued.

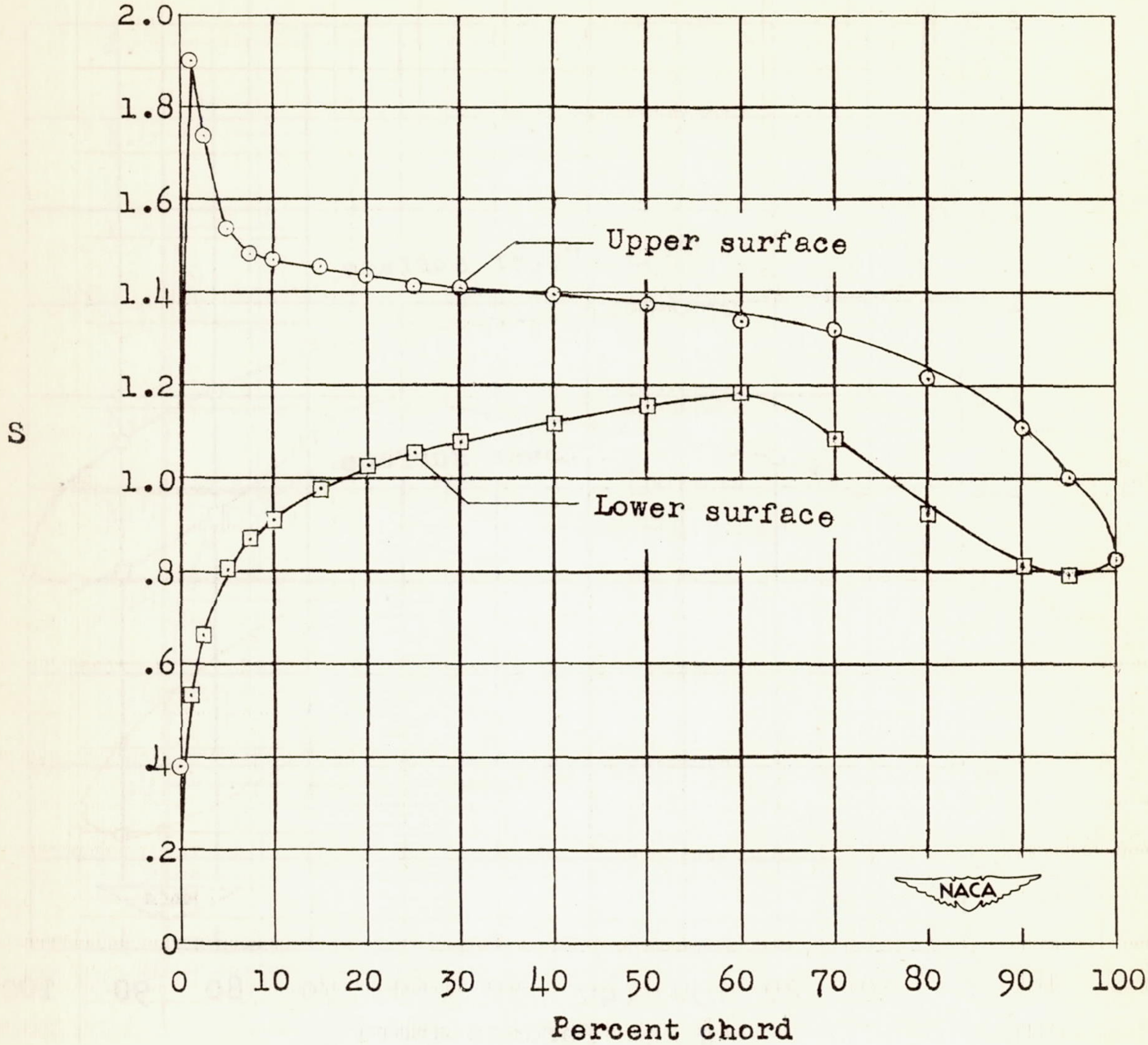

(o) $\alpha_o = 2.0^o$; $c_l = 0.37$.

Figure 6.- Continued.

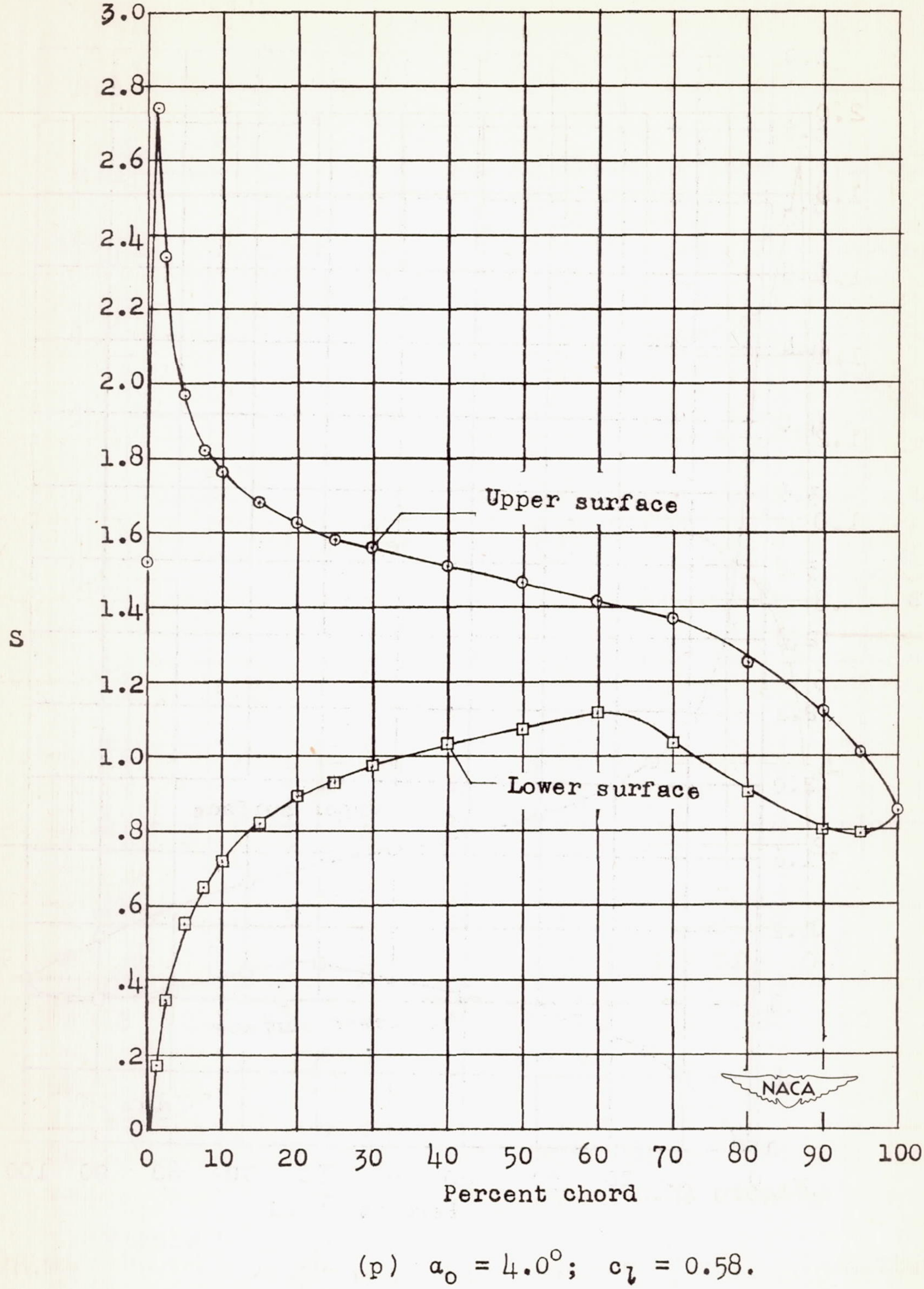

(p) $\alpha_o = 4.0^\circ$; $c_l = 0.58$.

Figure 6.- Continued.

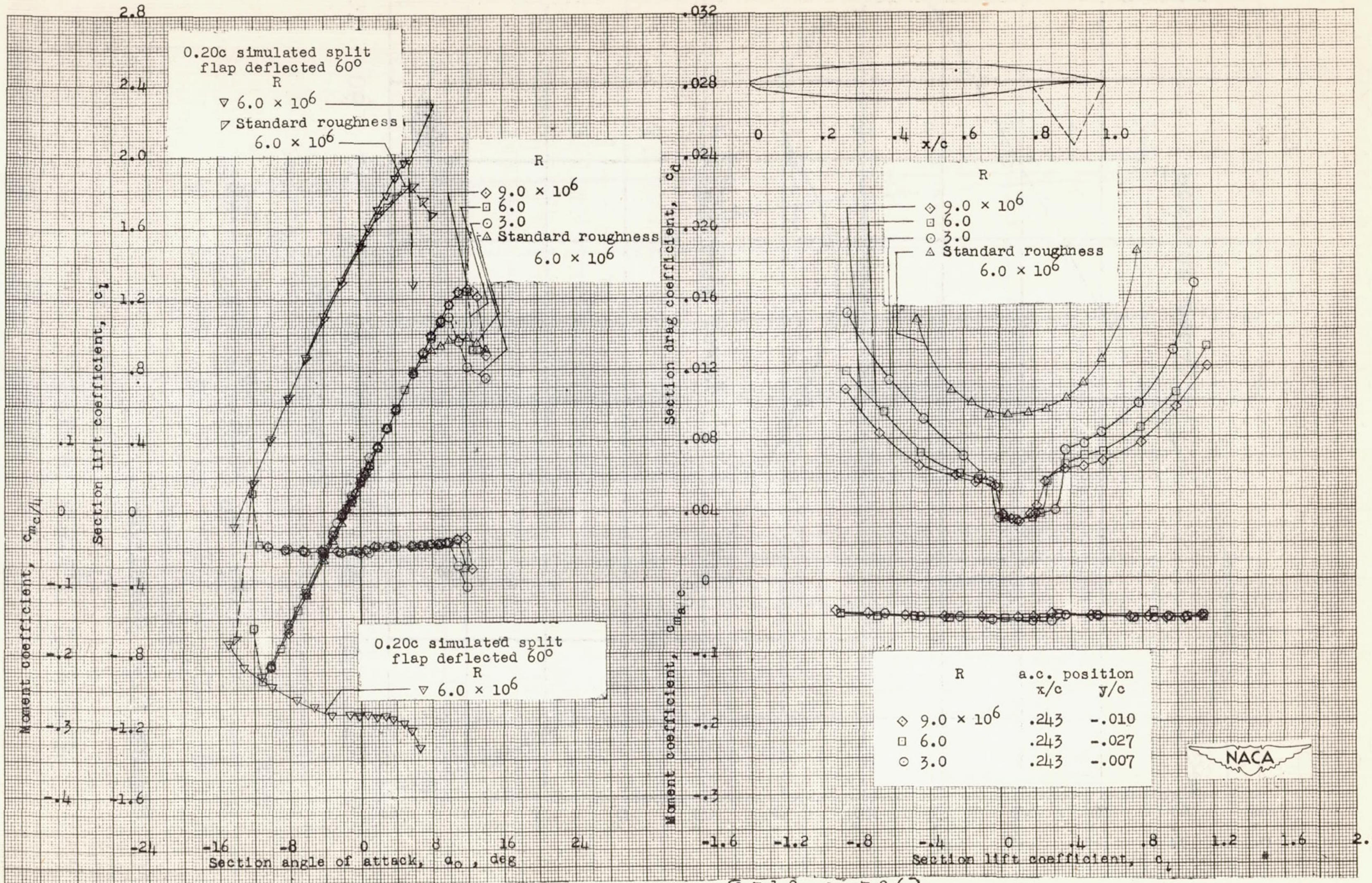

Figure 7.- Aerodynamic characteristics of the NACA $66_{(09)}$-210 $\left\{\begin{matrix} a = 1.0, & c_{l_i} = 0.6 \\ a = 0.6, & c_{l_i} = -0.4 \end{matrix}\right\}$ airfoil section, 24-inch chord.

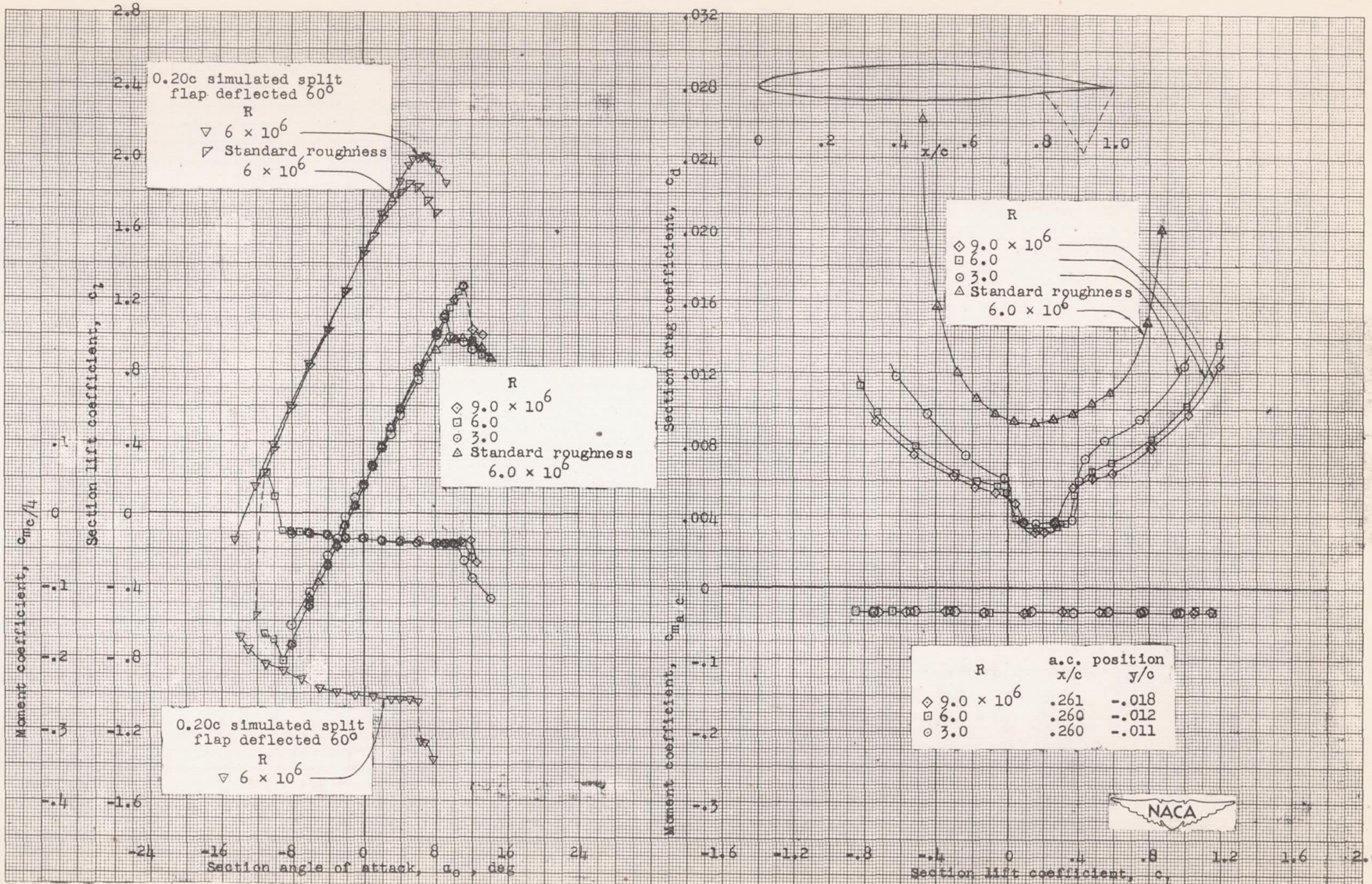

Figure 8.- Aerodynamic characteristics of the NACA 66-210 airfoil section, 24-inch chord.